

Ab initio Static Exchange–Correlation Kernel across Jacob’s Ladder without functional derivatives

Zhandos A. Moldabekov,^{1,2,*} Maximilian Böhme,^{1,2,3} Jan Vorberger,² David Blaschke,⁴ and Tobias Dornheim^{1,2,†}

¹Center for Advanced Systems Understanding (CASUS), D-02826 Görlitz, Germany

²Helmholtz-Zentrum Dresden-Rossendorf (HZDR), D-01328 Dresden, Germany

³Technische Universität Dresden, D-01062 Dresden, Germany

⁴Institute of Theoretical Physics, University of Wrocław, 50-204 Wrocław, Poland

The electronic exchange–correlation (XC) kernel constitutes a fundamental input for the estimation of a gamut of material properties such as the dielectric characteristics, the thermal and electrical conductivity, or the response to an external perturbation. In practice, no reliable method has been known that allows to compute the kernel of real materials with arbitrary XC functionals. In this work, we overcome this long-standing limitation by introducing a new, formally exact methodology for the computation of the material specific static XC kernel exclusively within the framework of density functional theory (DFT) and without employing functional derivatives—no external input apart from the usual XC-functional is required. We compare our new results with exact quantum Monte Carlo (QMC) data for the archetypical uniform electron gas model at both ambient and warm dense matter conditions. This gives us unprecedented insights into the performance of different XC-functionals, and has important implications for the development of new functionals that are designed for the application at extreme temperatures. In addition, we obtain new DFT results for the XC kernel of warm dense hydrogen as it occurs in fusion applications and astrophysical objects. The observed excellent agreement to the QMC reference data demonstrates that our framework is capable to capture nontrivial effects such as XC-induced isotropy breaking in the density response of hydrogen at large wave numbers.

The density functional theory (DFT) approach [1, 2] is arguably the most successful simulation tool in many-body physics, quantum chemistry, and related disciplines. Its main advantage is the evened out balance between reasonable accuracy and manageable computation cost, which allows for the *ab initio* description of real materials. While formally exact [3], DFT requires as external input the a-priori unknown exchange–correlation (XC) functional, which, in practice, has to be approximated. At ambient conditions, where the electrons are in the ground state, Jacob’s ladder of functionals [4, 5] serves as a useful categorization of different approximations, and the number of publications that utilize the DFT approach has been exponentially increasing over the last years [6].

The drastic reduction of the computation cost that renders DFT simulations feasible is achieved by a formally exact mapping onto an effective single-electron problem [3]. Unfortunately, the bulk of information about electron–electron correlations is lost in the process, and DFT gives straightforward access only to the single-electron density $n_e(\mathbf{r})$ and different contributions to the energy in practice; electron–electron correlations cannot be readily estimated. Therefore, advanced DFT applications such as linear-response time-dependent DFT (LR-TDDFT) [7] require as an additional input the material specific XC-kernel [8, 9] $K_{xc}(\mathbf{q}, \omega)$. Yet, very little is known about the actual XC-kernel of real materials [10, 11], and hitherto no feasible and universal way

to compute it has been known. In particular, there had been no possibility to compute the XC kernel for the existing great variety of XC functionals (more than 400) beyond the adiabatic LDA (ALDA) and GGA (AGGA) for extended systems [12].

In this Letter, we overcome these fundamental limitations by introducing a new, formally exact methodology for the *ab initio* calculation of the non-local static XC-kernel within the framework of DFT; it is fully compatible with the XC potential of selfconsistent Kohn–Sham (KS) equilibrium calculations for any XC functional. The presented approach completely circumvents the problem of computing functional derivatives, which had been the key obstacle that prevented going beyond AGGA for extended systems.

Specifically, we propose to use standard KS-DFT to compute the single-particle density $n_e(\mathbf{r})$ for a given electronic Hamiltonian \hat{H}_e . As a second step, we repeat the calculation for a modified Hamiltonian $\hat{H}_{\mathbf{q},A} = \hat{H}_e + \hat{V}_{\text{ext}}(\mathbf{q}, A)$ that is subject to a monochromatic external perturbation $\hat{V}_{\text{ext}}(\mathbf{q}, A) = 2A \sum_{j=1}^N \cos(\mathbf{q} \cdot \mathbf{r}_j)$ of wave vector \mathbf{q} and perturbation amplitude A [13–15]; this gives us the perturbed single-particle density $n_e(\mathbf{r})_{\mathbf{q},A}$. We can thus compute the induced density modulation as $\Delta n_e(\mathbf{r})_{\mathbf{q},A} = n_e(\mathbf{r})_{\mathbf{q},A} - n_e(\mathbf{r})$. In the limit of small A , the latter directly gives us the static linear density response function $\chi(\mathbf{q}) = \Delta n_e(\mathbf{r})_{\mathbf{q},A} / 2A \cos(\mathbf{q} \cdot \mathbf{r})$, which—in the general dynamic (i.e., $\omega \neq 0$) case—can be expressed for a homogeneous system (see the Supplemental Material [16] for more details) as [17, 18]

$$\chi(\mathbf{q}, \omega) = \frac{\chi_0(\mathbf{q}, \omega)}{1 - [v(q) + K_{xc}(\mathbf{q}, \omega)] \chi_0(\mathbf{q}, \omega)}. \quad (1)$$

* z.moldabekov@hzdr.de

† t.dornheim@hzdr.de

Here $v(q) = 4\pi/q^2$ is the Coulomb interaction, and $\chi_0(\mathbf{q}, \omega)$ denotes a known reference function, such as the Lindhard function in the case of a uniform electron gas (UEG) [18]. In this case, the XC-kernel, too, has a well-defined physical meaning and contains the full wave-vector- and frequency-resolved information about electronic XC-effects in the system. Moreover, it is then directly related to the *local field correction* $G(\mathbf{q}, \omega) = -K_{xc}(\mathbf{q}, \omega)/v(q)$ that is the central property within dielectric theories [19–24]. Hence, setting $K_{xc} \equiv 0$ leads to the mean-field level description, which is commonly known as the *random phase approximation* (RPA) [18], $\chi_{RPA}(\mathbf{q}, \omega)$. In the case of an inhomogeneous electron gas, for example in the potential of a fixed ion configuration, it is common practice to use the KS response function $\chi_{KS}(\mathbf{q}, \omega)$ as $\chi_0(\mathbf{q}, \omega)$ [25, 26]. As the final step, we invert Eq. (1) to compute the static XC-kernel $K_{xc}(\mathbf{q})$ for any given system.

To rigorously demonstrate the correctness and utility of our new approach, we consider two representative systems. The UEG [18, 27, 28] constitutes the archetypical electronic system and is the basis for many applications such as the BCS theory of superconductivity [29] and Fermi liquid theory [18]. As a second, even more challenging example, we consider hydrogen, the most abundant element in our universe, which is the subject of active investigation [10, 30–33]. We find excellent agreement with existing highly accurate quantum Monte Carlo (QMC) results [10, 14, 34] in both cases.

In addition, we analyze both the electronic ground state and so-called *warm dense matter* (WDM) at the electronic Fermi temperature, $\theta = k_B T/E_F = 1$ (with E_F being the usual Fermi energy [18]). In fact, WDM is ubiquitous in nature [35], and occurs in astrophysical objects such as giant planet interiors [36] and brown dwarfs [37]. Moreover, WDM is highly relevant for technological applications such as inertial confinement fusion [38] and the discovery of novel materials [39–41]. It is well-known that the theoretical description of WDM is notoriously difficult; from the perspective of DFT, one requires a density functional of the XC-free energy F_{xc} that explicitly depends on the electronic temperature T [42–44]. While first developments [45–48] have recently become available, the field of finite- T XC-functionals still remains in its infancy, and the performance of various approximations [49, 50] is substantially less understood compared to $T = 0$. Indeed, most DFT calculations for WDM are carried out on the basis of the *zero-temperature approximation* where the XC-free energy is approximated by the XC-energy in the ground state.

The main present limitation of our new approach is given by its restriction to compute the XC-kernel in the limit of $\omega = 0$. Still, it is possible to compute the dynamic density response function within the *static approximation* [51], i.e., by setting $K_{xc}(\mathbf{q}, \omega) \equiv K_{xc}(\mathbf{q})$ in Eq. (1). In this way, one combines a dynamic description on the level of the RPA with exact static correlations. This approximation has been shown to be highly accu-

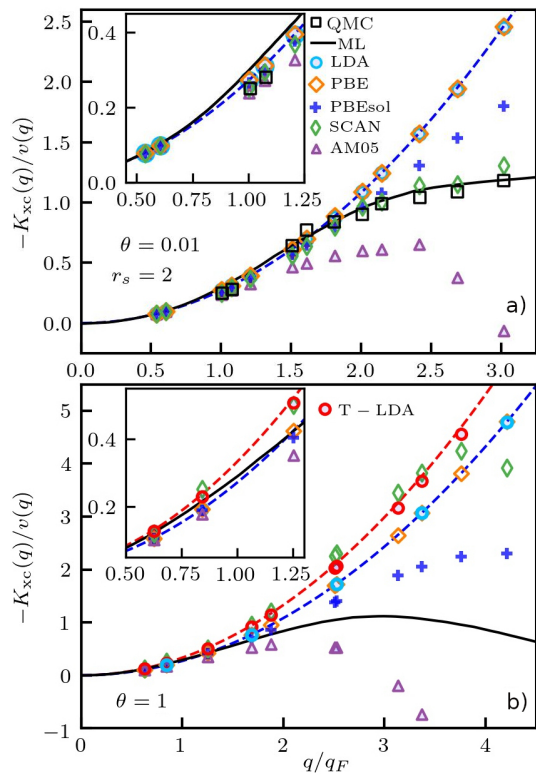


FIG. 1. XC-kernel $K_{xc}(\mathbf{q})$ of the UEG at a) ambient conditions with $\theta = 0.01$ and at b) WDM [53, 54] conditions with $\theta = 1$ for $r_s = 2$. Solid black line: exact UEG results based on the neural-net representation of Ref. [34]. Black squares: exact QMC results [14]. The other symbols distinguish DFT calculations for the density modulation using different XC-functionals.

rate in the case of the UEG for weak to moderate coupling strengths, including the important regime of metallic densities $r_s \lesssim 5$ (with r_s being the Wigner-Seitz radius in Hartree atomic units [52]).

Results. In Fig. 1a), we show the XC kernel of the UEG at $T = 0$ for the metallic density of $r_s = 2$. Specifically, we have carried out DFT calculations governed by the perturbed Hamiltonian for multiple wave vectors \mathbf{q} and a sufficiently small perturbation amplitude A ; the different symbols show results for a selection of popular XC-functionals. In addition, the solid black line corresponds to a parametrization [34] of the highly accurate QMC results by Moroni *et al.* [14] (black squares). Throughout this work, we follow the usual convention [34, 55, 56] and divide K_{xc} by the Coulomb interaction $v(q)$, resulting in the commonly analyzed local field correction. In the limit of small q , the LFC is known to satisfy the exact compressibility sum-rule [55], $\lim_{q \rightarrow 0} G(q) = -\frac{q^2}{4\pi} \partial^2 (nF_{xc}) / \partial n^2$, with $n = N/V$ being the average number density. It is depicted as the dashed blue parabola in Fig. 1a); we note that it holds $\lim_{T \rightarrow 0} F_{xc} = E_{xc}$. Evidently, $\lim_{q \rightarrow 0} G(q)$ is accurately reproduced both by the neural-net representation [34] and by all depicted XC-functionals for small q . Moreover,

both the LDA functional by Perdew and Wang [57] (light blue circles) and the generalized gradient approximation (GGA) by Perdew, Burke and Ernzerhof (PBE [58], orange diamonds) have been constructed to reproduce $\lim_{q \rightarrow 0} G(q)$ for all q [59] in the case of the UEG. This is substantiated by our empirical results and the LDA and PBE give indistinguishable results. Remarkably, the parabolic small- q expansion accurately reproduces the QMC data for $q \lesssim 2q_F$; this is a nontrivial observation which explains the success of both the simple LDA and the more sophisticated PBE in the description of bulk materials [14]. In contrast, the AM05 functional by Armiento and Mattson [60] (purple up-triangles), which is a semi-local GGA and has been shown to give comparable quality to hybrid functionals in the description of solids [61], only reproduces the QMC data for $q \lesssim 1.2q_F$. For large q , it has been designed to reproduce the Airy gas model [61], resulting in a substantial drop towards negative values. The semi-empirical PBEsol [62] (blue plusses), on the other hand, is virtually indistinguishable from PBE for $q \lesssim 2q_F$, and exhibits a somewhat higher accuracy at large wavenumbers. Finally, the meta-GGA SCAN [63] (green diamonds) constitutes by far the most accurate functional for the ground state and gives basically exact results over the entire depicted q -range, as it was designed to reproduce the QMC results [63].

In Fig. 1b), we present results for the UEG in the WDM regime, i.e., at the electronic Fermi temperature $\theta = 1$. In this case, we additionally consider the finite- T LDA functional by Groth *et al.* [46] (red circles). The dashed red and blue lines show the exact small- q expansion $\lim_{q \rightarrow 0} G(q)$ evaluated at $\theta = 1$ and $\theta = 0$, respectively. Evidently, the ground-state LDA (and PBE) follows the latter curve, as it is expected. Similarly, the finite- T LDA follows the red curve and, therefore, reproduces the correct impact of the temperature on the small- q limit. This can be seen particularly well in the inset where we show a magnified segment. It can be expected that the recent finite- T GGA functional [47] exhibits the same behavior as it has been constructed to reproduce the finite- T LDA for the UEG. In practice, however, the impact of $K_{xc}(\mathbf{q})$ on the density response function vanishes for $q \rightarrow 0$, and even the RPA becomes exact. For $q \gtrsim q_F$, where the impact of the XC-kernel is most pronounced, the ground-state evaluation of $\lim_{q \rightarrow 0} G(q)$ coincidentally constitutes a superior approximation to the true curve (solid black). Therefore, the ground-state LDA exhibits a better accuracy than the consistently temperature-dependent functional. This is a very important point for which a more detailed analysis for $1 \leq r_s \leq 6$ and $0 \leq \theta \leq 4$ is presented in the Supplementary Material [16].

We stress that these findings have profound consequences for the construction of the next generation of XC-functionals that are specifically designed for the application at WDM conditions. Evidently, translating Jacob’s ladder of functional approximations [4] from the ground-state to finite temperatures does not nec-

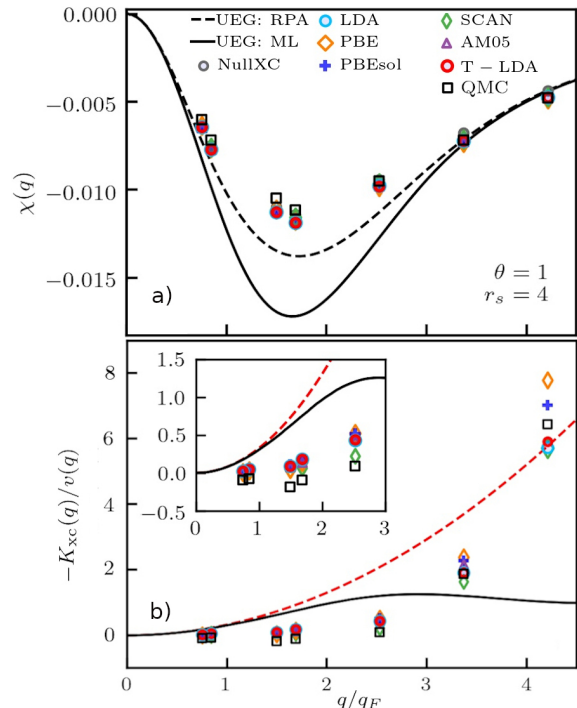


FIG. 2. a) Electronic static density response function $\chi(\mathbf{q})$ and b) XC-kernel $K_{xc}(\mathbf{q})$ (bottom panel) of hydrogen at WDM [53, 54] conditions ($\theta = 1$) for $r_s = 4$. Solid (dashed) black line: exact results for the UEG model at the same conditions based on the neural-net representation of Ref. [34] (analytical RPA). Black squares: exact QMC results for hydrogen [10]. The other symbols distinguish DFT calculations for the density modulation using different XC-functionals.

essarily improve the quality of DFT simulations in the WDM regime. Making the lowest rung—i.e., the LDA—explicitly T -dependent might actually lead to a deterioration of the attained accuracy. Moreover, this deficiency is, by design, not removed on the GGA-level, which is based on the same $q \rightarrow 0$ expansion.

Returning to Fig. 1b), we find that the ground-state SCAN functional performs similarly poorly as AM05, which is in stark contrast to its impressive accuracy at $T = 0$. We thus conclude that the meta-GGA corrections on which SCAN is based strongly depend on the electronic temperature. In contrast, the semi-empirical PBEsol provides a more accurate description of the static XC kernel at $q \lesssim 2.5q_F$ than LDA, T-LDA, AM05, and SCAN.

Let us next consider hydrogen at extreme conditions—a state of matter that plays a central role in the description of the implosion path of a fuel capsule towards nuclear fusion [38] and naturally occurs within astrophysical objects such as giant planet interiors [36]. In Fig. 2, we show our new DFT results for the static density response of hydrogen that has been computed for a single fixed ion snapshot from a corresponding DFT-MD simulation. We note that, while the averaging over many snapshots is straightforward, benchmarking DFT for a single pro-

ton configuration constitutes an even more rigorous test of our methodology as, in this way, error cancellation between different snapshots is ruled out.

At $r_s = 2$, where hydrogen is known to be mostly ionized, the bulk of the electrons can be categorized as *unbound*, meaning that they are not primarily localized around the protons. Therefore, the density response closely resembles the UEG model and we find the same conclusions as in Fig. 1a), see the Supplemental Material [16].

From a physical perspective, the case of $r_s = 4$ shown in Fig. 2 is more interesting. In addition to the more pronounced impact of Coulomb correlations, hydrogen is partially ionized at these conditions, with an approximate fraction of *free electrons* of $\alpha = 0.54 - 0.6$ [10, 64]. Consequently, the numerical results for $\chi(\mathbf{q})$, Fig. 2a), exhibit a substantially reduced density response compared to the UEG, as the *bound* electrons cannot react as much as the free electrons to the external potential. Overall, we find good qualitative agreement between DFT and the QMC data over the entire depicted q -range, even though the true reduction of the density response due to the localization around the protons is somewhat underestimated for $q_F \lesssim q \lesssim 3q_F$. Remarkably, we find that all XC-functionals reproduce the nontrivial increase in the magnitude of $\chi(\mathbf{q})$ compared to the UEG model around $q \sim 4q_F$, which has been explained as a consequence of isotropy breaking in the presence of the proton configuration in Ref. [10].

In Fig. 2b), we show the corresponding XC-kernels, that we have extracted from the different $\chi(\mathbf{q})$ data sets via Eq. (1). As the reference function, we use a mean-field response function $\chi_0(\mathbf{q})$ that we have obtained from a separate DFT simulation with the XC-functional being set to zero. This has the advantage that XC-kernels from different theories are directly comparable to each other. For completeness, we note that extracting the actual XC-functional dependent kernel by inserting the respective $\chi_{\text{KS}}(\mathbf{q}, 0)$ into Eq. (1) is straightforward, but would make the direct comparison less meaningful. The resulting data for $K_{\text{xc}}(\mathbf{q})$ of hydrogen at $r_s = 4$ and $\theta = 1$ qualitatively agree with each other, but starkly disagree from the UEG model at these conditions. In particular, the kernel attains remarkably small values for $q \lesssim 2.5q_F$, followed by a pronounced increase for $q \gtrsim 3q_F$. Clearly, our new methodology is capable to accurately capture the complex interplay of the ion structure with electronic XC-effects as they manifest in $K_{\text{xc}}(\mathbf{q})$. In addition, we do not find the simple parabolic behaviour for $\lim_{q \rightarrow 0} G(q)$ from LDA. In fact, $K_{\text{xc}}(\mathbf{q})$ from the ALDA always reduces to a constant, leading to $G(q) \sim q^2$ [12, 65]. In our method, the total response of a system to a harmonic perturbation with a given wave vector is self-consistently determined by the electron density everywhere in the simulation cell.

Let us conclude this analysis of the static density response of warm dense hydrogen by comparing our new approach to the current state-of-the-art. In Fig. 3,

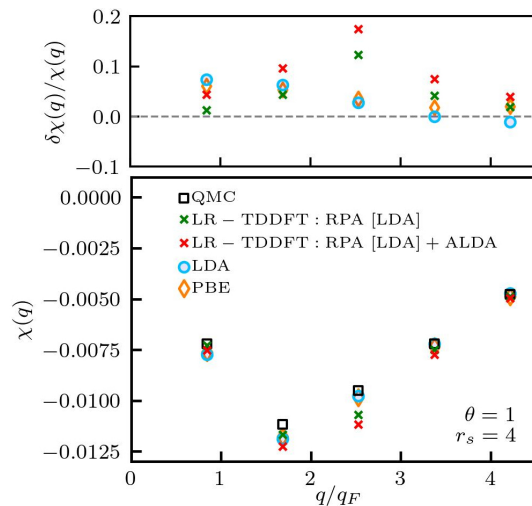


FIG. 3. Illustration of the inconsistent combination of $\chi_{\text{KS}}(\mathbf{q}, \omega)$ with the ALDA kernel. Bottom: Static density response of warm dense hydrogen with $r_s = 4$ and $\theta = 1$; the light blue circles, orange diamonds, and black squares are taken from Fig. 2. Green crosses: Static ($\omega \rightarrow 0$) limit of LR-TDDFT results within RPA based on $\chi_{\text{KS}}(\mathbf{q}, \omega)$ using KS-orbitals from a ground-state LDA calculation. Red crosses: corresponding ALDA results. Top panel: relative error with respect to exact QMC benchmark data. The inconsistent incorporation of the ALDA model kernel leads to a deterioration compared to RPA for all depicted q .

again consider hydrogen at $r_s = 4$ and $\theta = 1$, and the black squares, blue circles, and orange triangles show the QMC, LDA, and PBE results from Fig. 2. In addition, the green crosses have been obtained following the standard paradigm within LR-TDDFT, that is, computing the reference function $\chi_0(\mathbf{q}, \omega)$ in the limit of $\omega \rightarrow 0$ on the basis of the KS-orbitals from a DFT simulation of the unperturbed system using the LDA functional. Both the KS-response function and the corresponding RPA are de-facto uncontrolled approximations. In practice, the green crosses are accurate for small q , but lead to a substantial deterioration in the accuracy for $q \gtrsim 2q_F$ compared to the LDA evaluation proposed in the present work; this can be seen particularly well in the top panel showing a the relative deviation to the exact QMC reference data. Even worse, including the widely used ALDA model as the XC-kernel (red crosses)—a standard practice within LR-TDDFT [25, 26]—*actually increases the systematic errors* for all q . This constitutes an unambiguous demonstration of the practical impact of the inconsistent combination of a KS-response function with an XC-kernel from a different model, which is overcome by our new approach.

Discussion. We have presented a new, formally exact framework to compute the material specific electronic static XC-kernel within DFT, and without any additional external input apart from the usual XC-functional. Our methodology provides access to the static XC kernel across all rungs of Jacob’s ladder, including promising

hybrid functionals [66]. The analysis of the XC-kernel $K_{xc}(\mathbf{q})$ on the basis of a particular functional can give valuable insights to guide new developments, as we have demonstrated for the case of WDM. Beyond WDM, the presented framework will have a strong impact on a number of research fields within physics, chemistry, and related disciplines. Indeed, the XC-kernel is the key ingredient to a host of practical applications, such as the construction of electronically screened effective potentials [18, 67, 68], the incorporation of correlation effects into quantum fluid dynamics [69–71], and the estimation of the energy loss characteristics of high-energy density plasmas [72–74]. A particularly important example is given by the interpretation of XRTS experiments within the widely used Chihara approximation [75, 76]. Moreover, the fluctuation–dissipation theorem gives a direct relation between the thus obtained density response and the dynamic structure factor $S_{ee}(\mathbf{q}, \omega)$. Consequently,

our new framework for the XC-kernel opens up the exciting possibility to obtain the static structure factor $S_{ee}(\mathbf{q})$ —the Fourier transform of the pair correlation function $g_{ee}(\mathbf{r})$ —of two electrons *exclusively within DFT and without any additional external input* apart from the usual XC-functional of standard DFT.

ACKNOWLEDGMENTS

We gratefully acknowledge helpful comments by K. Burke (UC Irvine). This work was partially supported by the Center for Advanced Systems Understanding (CASUS) which is financed by Germany’s Federal Ministry of Education and Research (BMBF) and by the Saxon state government out of the State budget approved by the Saxon State Parliament. D.B. acknowledges support by the Polish National Science Center (NCN) under grant No. 2019/33/B/ST9/03059.

-
- [1] R. O. Jones and O. Gunnarsson, “The density functional formalism, its applications and prospects,” *Rev. Mod. Phys.* **61**, 689–746 (1989).
- [2] R. O. Jones, “Density functional theory: Its origins, rise to prominence, and future,” *Reviews of Modern Physics* **87**, 897–923 (2015).
- [3] P. Hohenberg and W. Kohn, “Inhomogeneous electron gas,” *Phys. Rev.* **136**, B864–B871 (1964).
- [4] John P. Perdew and Karla Schmidt, “Jacob’s ladder of density functional approximations for the exchange–correlation energy,” *AIP Conference Proceedings* **577**, 1–20 (2001).
- [5] Jianmin Tao, John P. Perdew, Viktor N. Staroverov, and Gustavo E. Scuseria, “Climbing the density functional ladder: Nonempirical Meta–Generalized gradient approximation designed for molecules and solids,” *Physical Review Letters* **91**, 146401 (2003).
- [6] Aurora Pribram-Jones, David A. Gross, and Kieron Burke, “DFT: A theory full of holes?” *Annual Review of Physical Chemistry* **66**, 283–304 (2015).
- [7] M. Petersilka, U. J. Gossmann, and E. K. U. Gross, “Excitation energies from time-dependent density-functional theory,” *Phys. Rev. Lett.* **76**, 1212–1215 (1996).
- [8] Andreas Görling, “Hierarchies of methods towards the exact kohn-sham correlation energy based on the adiabatic-connection fluctuation-dissipation theorem,” *Phys. Rev. B* **99**, 235120 (2019).
- [9] Andreas Görling, “Exact exchange–correlation kernel for dynamic response properties and excitation energies in density-functional theory,” *Phys. Rev. A* **57**, 3433–3436 (1998).
- [10] Maximilian Böhme, Zhandos A. Moldabekov, Jan Vorberger, and Tobias Dornheim, “Static electronic density response of warm dense hydrogen: Ab initio path integral monte carlo simulations,” *Phys. Rev. Lett.* **129**, 066402 (2022).
- [11] Maximilian Böhme, Zhandos A. Moldabekov, Jan Vorberger, and Tobias Dornheim, “Ab initio path integral monte carlo simulations of hydrogen snapshots at warm dense matter conditions,” (2022).
- [12] Young-Moo Byun, Jiuyu Sun, and Carsten A Ullrich, “Time-dependent density-functional theory for periodic solids: assessment of excitonic exchange–correlation kernels,” *Electronic Structure* **2**, 023002 (2020).
- [13] S. Moroni, D. M. Ceperley, and G. Senatore, “Static response from quantum Monte Carlo calculations,” *Phys. Rev. Lett* **69**, 1837 (1992).
- [14] S. Moroni, D. M. Ceperley, and G. Senatore, “Static response and local field factor of the electron gas,” *Phys. Rev. Lett* **75**, 689 (1995).
- [15] Tobias Dornheim, Jan Vorberger, and Michael Bonitz, “Nonlinear electronic density response in warm dense matter,” *Physical Review Letters* **125**, 085001 (2020).
- [16] “Supplemental material,” (2022), published online.
- [17] A. A. Kugler, “Theory of the local field correction in an electron gas,” *J. Stat. Phys* **12**, 35 (1975).
- [18] G. Giuliani and G. Vignale, *Quantum theory of the electron liquid* (Cambridge University Press, Cambridge, 2008).
- [19] K. S. Singwi, M. P. Tosi, R. H. Land, and A. Sjölander, “Electron correlations at metallic densities,” *Phys. Rev* **176**, 589 (1968).
- [20] S. Tanaka and S. Ichimaru, “Thermodynamics and correlational properties of finite-temperature electron liquids in the Singwi-Tosi-Land-Sjölander approximation,” *J. Phys. Soc. Jpn* **55**, 2278–2289 (1986).
- [21] P. Vashishta and K. S. Singwi, “Electron correlations at metallic densities v,” *Physical Review B* **6**, 875 (1972).
- [22] A. Holas and S. Rahman, “Dynamic local-field factor of an electron liquid in the quantum versions of the Singwi-Tosi-Land-Sjölander and Vashishta-Singwi theories,” *Physical Review B* **35**, 2720 (1987).
- [23] P. Tolias, F. Lucco Castello, and T. Dornheim, “Integral equation theory based dielectric scheme for strongly coupled electron liquids,” *The Journal of Chemical Physics* **155**, 134115 (2021).
- [24] S. Tanaka, “Correlational and thermodynamic properties of finite-temperature electron liquids in the hypernetted-

- chain approximation,” *J. Chem. Phys.* **145**, 214104 (2016).
- [25] C. Ullrich, *Time-Dependent Density-Functional Theory: Concepts and Applications*, Oxford Graduate Texts (OUP Oxford, 2012).
- [26] M.A.L. Marques, N.T. Maitra, F.M.S. Nogueira, E.K.U. Gross, and A. Rubio, *Fundamentals of Time-Dependent Density Functional Theory*, Lecture Notes in Physics (Springer Berlin Heidelberg, 2012).
- [27] P.-F. Loos and P. M. W. Gill, “The uniform electron gas,” *Comput. Mol. Sci* **6**, 410–429 (2016).
- [28] T. Dornheim, S. Groth, and M. Bonitz, “The uniform electron gas at warm dense matter conditions,” *Physics Reports* **744**, 1 – 86 (2018).
- [29] J. Bardeen, L. N. Cooper, and J. R. Schrieffer, “Theory of superconductivity,” *Physical Review* **108**, 1175–1204 (1957), number of pages: 0 Publisher: American Physical Society.
- [30] Jeffrey M. McMahon, Miguel A. Morales, Carlo Pierleoni, and David M. Ceperley, “The properties of hydrogen and helium under extreme conditions,” *Reviews of Modern Physics* **84**, 1607–1653 (2012).
- [31] Carlo Pierleoni, Miguel A. Morales, Giovanni Rillo, Markus Holzmann, and David M. Ceperley, “Liquid–liquid phase transition in hydrogen by coupled electron–ion monte carlo simulations,” *Proceedings of the National Academy of Sciences* **113**, 4953–4957 (2016).
- [32] Ranga P. Dias and Isaac F. Silvera, “Observation of the wigner-huntington transition to metallic hydrogen,” *Science* **355**, 715–718 (2017).
- [33] Peter M. Celliers, Marius Millot, Stephanie Brygoo, R. Stewart McWilliams, Dayne E. Fratanduono, J. Ryan Rygg, Alexander F. Goncharov, Paul Loubeyre, Jon H. Eggert, J. Luc Peterson, Nathan B. Meezan, Sebastien Le Pape, Gilbert W. Collins, Raymond Jeanloz, and Russell J. Hemley, “Insulator-metal transition in dense fluid deuterium,” *Science* **361**, 677–682 (2018).
- [34] T. Dornheim, J. Vorberger, S. Groth, N. Hoffmann, Zh.A. Moldabekov, and M. Bonitz, “The static local field correction of the warm dense electron gas: An ab initio path integral Monte Carlo study and machine learning representation,” *J. Chem. Phys.* **151**, 194104 (2019).
- [35] V. E. Fortov, “Extreme states of matter on Earth and in space,” *Phys.-Usp* **52**, 615–647 (2009).
- [36] Alessandra Benuzzi-Mounaix, Stéphane Mazevet, Alessandra Ravasio, Tommaso Vinci, Adrien Denoed, Michel Koenig, Nourou Amadou, Erik Brambrink, Floriane Festa, Anna Levy, Marion Harmand, Stéphanie Brygoo, Gael Huser, Vanina Recoules, Johan Bouchet, Guillaume Morard, François Guyot, Thibaut de Resseguier, Kohei Myanishi, Norimasa Ozaki, Fabien Dorchies, Jérôme Gaudin, Pierre Marie Leguay, Olivier Peyrusse, Olivier Henry, Didier Raffestin, Sebastien Le Pape, Ray Smith, and Riccardo Musella, “Progress in warm dense matter study with applications to planetology,” *Physica Scripta* **T161**, 014060 (2014), publisher: IOP Publishing.
- [37] A. Becker, W. Lorenzen, J. J. Fortney, N. Nettelmann, M. Schöttler, and R. Redmer, “Ab initio equations of state for hydrogen (H-REOS.3) and helium (He-REOS.3) and their implications for the interior of brown dwarfs,” *Astrophys. J. Suppl. Ser* **215**, 21 (2014).
- [38] S. X. Hu, B. Militzer, V. N. Goncharov, and S. Skupsky, “First-principles equation-of-state table of deuterium for inertial confinement fusion applications,” *Physical Review B* **84**, 224109 (2011).
- [39] A. Lazicki, D. McGonegle, J. R. Rygg, D. G. Braun, D. C. Swift, M. G. Gorman, R. F. Smith, P. G. Heighway, A. Higginbotham, M. J. Suggit, D. E. Fratanduono, F. Coppari, C. E. Wehrenberg, R. G. Kraus, D. Erskine, J. V. Bernier, J. M. McNaney, R. E. Rudd, G. W. Collins, J. H. Eggert, and J. S. Wark, “Metastability of diamond ramp-compressed to 2 terapascals,” *Nature* **589**, 532–535 (2021).
- [40] D. Kraus, J. Vorberger, A. Pak, N. J. Hartley, L. B. Fletcher, S. Frydrych, E. Galtier, E. J. Gamboa, D. O. Gericke, S. H. Glenzer, E. Granados, M. J. MacDonald, A. J. MacKinnon, E. E. McBride, I. Nam, P. Neumayer, M. Roth, A. M. Saunders, A. K. Schuster, P. Sun, T. van Driel, T. Döppner, and R. W. Falcone, “Formation of diamonds in laser-compressed hydrocarbons at planetary interior conditions,” *Nature Astronomy* **1**, 606–611 (2017).
- [41] D. Kraus, A. Ravasio, M. Gauthier, D. O. Gericke, J. Vorberger, S. Frydrych, J. Helfrich, L. B. Fletcher, G. Schaubmann, B. Nagler, B. Barbrel, B. Bachmann, E. J. Gamboa, S. Göde, E. Granados, G. Gregori, H. J. Lee, P. Neumayer, W. Schumaker, T. Döppner, R. W. Falcone, S. H. Glenzer, and M. Roth, “Nanosecond formation of diamond and lonsdaleite by shock compression of graphite,” *Nature Communications* **7**, 10970 (2016).
- [42] N. David Mermin, “Thermal properties of the inhomogeneous electron gas,” *Physical Review* **137**, A1441–A1443 (1965).
- [43] V. V. Karasiev, L. Calderin, and S. B. Trickey, “Importance of finite-temperature exchange correlation for warm dense matter calculations,” *Physical Review E* **93**, 063207 (2016).
- [44] Kushal Ramakrishna, Tobias Dornheim, and Jan Vorberger, “Influence of finite temperature exchange-correlation effects in hydrogen,” *Phys. Rev. B* **101**, 195129 (2020).
- [45] Valentin V. Karasiev, Travis Sjostrom, James Dufty, and S. B. Trickey, “Accurate homogeneous electron gas exchange-correlation free energy for local spin-density calculations,” *Physical Review Letters* **112**, 076403 (2014).
- [46] Simon Groth, Tobias Dornheim, Travis Sjostrom, Fionn D. Malone, W. M. C. Foulkes, and Michael Bonitz, “Ab initio Exchange-Correlation Free Energy of the Uniform Electron Gas at Warm Dense Matter Conditions,” *Physical Review Letters* **119**, 135001 (2017), publisher: American Physical Society.
- [47] Valentin V. Karasiev, James W. Dufty, and S. B. Trickey, “Nonempirical semilocal free-energy density functional for matter under extreme conditions,” *Physical Review Letters* **120**, 076401 (2018).
- [48] D. I. Mihaylov, V. V. Karasiev, and S. X. Hu, “Thermal hybrid exchange-correlation density functional for improving the description of warm dense matter,” *Physical Review B* **101**, 245141 (2020), number of pages: 6 Publisher: American Physical Society.
- [49] Zhandos Moldabekov, Tobias Dornheim, Maximilian Böhme, Jan Vorberger, and Attila Cangi, “The relevance of electronic perturbations in the warm dense electron gas,” *The Journal of Chemical Physics* **155**, 124116 (2021).
- [50] Zhandos Moldabekov, Tobias Dornheim, Jan Vorberger,

- and Attila Cangi, “Benchmarking exchange-correlation functionals in the spin-polarized inhomogeneous electron gas under warm dense conditions,” *Phys. Rev. B* **105**, 035134 (2022).
- [51] T. Dornheim, S. Groth, J. Vorberger, and M. Bonitz, “Ab initio path integral Monte Carlo results for the dynamic structure factor of correlated electrons: From the electron liquid to warm dense matter,” *Physical Review Letters* **121**, 255001 (2018).
- [52] Torben Ott, Hauke Thomsen, Jan Willem Abraham, Tobias Dornheim, and Michael Bonitz, “Recent progress in the theory and simulation of strongly correlated plasmas: phase transitions, transport, quantum, and magnetic field effects,” *The European Physical Journal D* **72**, 84 (2018).
- [53] M. Bonitz, T. Dornheim, Zh. A. Moldabekov, S. Zhang, P. Hamann, H. Kählert, A. Filinov, K. Ramakrishna, and J. Vorberger, “Ab initio simulation of warm dense matter,” *Physics of Plasmas* **27**, 042710 (2020).
- [54] F. Graziani, M. P. Desjarlais, R. Redmer, and S. B. Trickey, eds., *Frontiers and challenges in warm dense matter* (Springer, International Publishing, 2014).
- [55] Setsuo Ichimaru, Hiroshi Iyetomi, and Shigenori Tanaka, “Statistical physics of dense plasmas: Thermodynamics, transport coefficients and dynamic correlations,” *Physics Reports* **149**, 91–205 (1987).
- [56] M. Corradini, R. Del Sole, G. Onida, and M. Palumbo, “Analytical expressions for the local-field factor $G(q)$ and the exchange-correlation kernel $K_{xc}(r)$ of the homogeneous electron gas,” *Physical Review B* **57**, 14569 (1998).
- [57] John P. Perdew and Yue Wang, “Accurate and simple analytic representation of the electron-gas correlation energy,” *Phys. Rev. B* **45**, 13244–13249 (1992).
- [58] John P. Perdew, Kieron Burke, and Matthias Ernzerhof, “Generalized gradient approximation made simple,” *Physical Review Letters* **77**, 3865–3868 (1996).
- [59] J. P. Perdew, D. C. Langreth, and V. Sahni, “Corrections to the local density approximation: Gradient expansion versus wave-vector analysis for the metallic surface problem,” *Phys. Rev. Lett.* **38**, 1030–1033 (1977).
- [60] R. Armiento and A. E. Mattsson, “Functional designed to include surface effects in self-consistent density functional theory,” *Physical Review B* **72**, 085108 (2005).
- [61] Ann E. Mattsson, Rickard Armiento, Joachim Paier, Georg Kresse, John M. Wills, and Thomas R. Mattsson, “The AM05 density functional applied to solids,” *The Journal of Chemical Physics* **128**, 084714 (2008).
- [62] John P. Perdew, Adrienn Ruzsinszky, Gábor I. Csonka, Oleg A. Vydrov, Gustavo E. Scuseria, Lucian A. Constantin, Xiaolan Zhou, and Kieron Burke, “Restoring the density-gradient expansion for exchange in solids and surfaces,” *Physical Review Letters* **100**, 136406 (2008).
- [63] Jianwei Sun, Adrienn Ruzsinszky, and John P. Perdew, “Strongly constrained and appropriately normed semilocal density functional,” *Physical Review Letters* **115**, 036402 (2015).
- [64] B. Militzer and D. M. Ceperley, “Path integral monte carlo simulation of the low-density hydrogen plasma,” *Phys. Rev. E* **63**, 066404 (2001).
- [65] Mark S. Hybertsen and Steven G. Louie, “Ab initio static dielectric matrices from the density-functional approach. i. formulation and application to semiconductors and insulators,” *Phys. Rev. B* **35**, 5585–5601 (1987).
- [66] Jochen Heyd, Gustavo E. Scuseria, and Matthias Ernzerhof, “Hybrid functionals based on a screened Coulomb potential,” *The Journal of Chemical Physics* **118**, 8207–8215 (2003).
- [67] G. Senatore, S. Moroni, and D. M. Ceperley, “Local field factor and effective potentials in liquid metals,” *J. Non-Cryst. Sol* **205-207**, 851–854 (1996).
- [68] Zh.A. Moldabekov, H. Kählert, T. Dornheim, S. Groth, M. Bonitz, and T. S. Ramazanov, “Dynamical structure factor of strongly coupled ions in a dense quantum plasma,” *Physical Review E* **99**, 053203 (2019).
- [69] A. Diaw and M.S. Murillo, “A viscous quantum hydrodynamics model based on dynamic density functional theory,” *Sci. Reports* **7**, 15352 (2017).
- [70] Zh. A. Moldabekov, M. Bonitz, and T. S. Ramazanov, “Theoretical foundations of quantum hydrodynamics for plasmas,” *Physics of Plasmas* **25**, 031903 (2018).
- [71] Z. A. Moldabekov, T. Dornheim, G. Gregori, F. Graziani, M. Bonitz, and A. Cangi, “Towards a Quantum Fluid Theory of Correlated Many-Fermion Systems from First Principles,” *SciPost Phys.* **12**, 62 (2022).
- [72] D.O Gericke, M Schlages, and W.D Kraeft, “Stopping power of a quantum plasma — t-matrix approximation and dynamical screening,” *Physics Letters A* **222**, 241–245 (1996).
- [73] Zh. A. Moldabekov, T. Dornheim, M. Bonitz, and T. S. Ramazanov, “Ion energy-loss characteristics and friction in a free-electron gas at warm dense matter and non-ideal dense plasma conditions,” *Phys. Rev. E* **101**, 053203 (2020).
- [74] Y. H. Ding, A. J. White, S. X. Hu, O. Certik, and L. A. Collins, “Ab initio studies on the stopping power of warm dense matter with time-dependent orbital-free density functional theory,” *Physical Review Letters* **121**, 145001 (2018).
- [75] J Chihara, “Difference in x-ray scattering between metallic and non-metallic liquids due to conduction electrons,” *Journal of Physics F: Metal Physics* **17**, 295–304 (1987).
- [76] D. Kraus, B. Bachmann, B. Barbrel, R. W. Falcone, L. B. Fletcher, S. Frydrych, E. J. Gamboa, M. Gauthier, D. O. Gericke, S. H. Glenzer, S. Göde, E. Granados, N. J. Hartley, J. Helfrich, H. J. Lee, B. Nagler, A. Ravasio, W. Schumaker, J. Vorberger, and T. Döppner, “Characterizing the ionization potential depression in dense carbon plasmas with high-precision spectrally resolved x-ray scattering,” *Plasma Phys. Control Fusion* **61**, 014015 (2019).